Supporting Information for

Sustainable valorization of mandarin peel waste into multifunctional cellulose/pectin/PVA films with superior mechanical and UV-blocking performance

Yongjun Cho[1], Sunoo Hwang[1], Pham Thanh Trung Ninh[1], Youngju Kim[1], Shinhyeong Choe[1], Jaewook Myung[1*]

[1] Department of Civil and Environmental Engineering, KAIST, Daejeon 34141, Republic of Korea

*Corresponding author: Jaewook Myung

Email: jjaimyung@kaist.ac.kr

This material includes:

Characterization methods

Supplementary tables

Table S1. Elemental analysis for biodegradation test samples

Table S2. Characteristic FT-IR peak assignments

Table S3. Pectin, cellulose, and lignin content in mandarin peel waste

Table S4. Summary of the mechanical and optical properties of the prepared M/P films

Table S5. Comparison of the mechanical properties and optical properties with other PVA/biomass composite film examples

Supplementary figures

Fig. S1. Proposed structure of the mandarin peel/PVA blend films.

Fig. S2. Experimental scheme employing different pretreatment methods.

Fig. S3. Detailed procedure for Delig-1:1 sample preparation.

Fig. S4. Surface morphology of the blend films.

Fig. S5. Determination of onset temperatures from TGA curves.

Fig. S6. Foldability and flexibility of Na_2CO_3-1:1-W film.

Fig. S7. Water contact angle results of M/P and PVA films.

Fig. S8. Representative photos of simulated soil degradation test.

Fig. S9. Additional SEM images of Na_2CO_3-1:1-W film after 4 months of immersion in river water.

References

Characterization methods

Chemical composition analysis of mandarin peel powder. Cellulose, pectin, and lignin compositions were determined according to extraction methods in the literature.[1] Pectin extraction was performed by using 3 mg/mL citric acid solution, reacted at 90 °C for 30 minutes. The solution was centrifuged to collect insoluble cellulose and lignin fraction, followed by precipitation of filtrate using 96 vol% ethanol solution for 24 hours. Precipitated pectin was collected by centrifugation, dried, and weighed. Cellulose was extracted by consecutive water extraction, acid hydrolysis, alkaline hydrolysis, and $NaClO_2$ bleaching. All procedures except water extraction were repeated twice. Lignin content was determined based on the TAPPI standard.[2] Briefly, 1 g of mandarin peel powder was hydrolyzed by 20 mL of 72 wt% sulfuric acid for 2 hours. The solution was then diluted with 750 mL of water and then further reacted for 4 hours at boiling temperature. The precipitated acid-insoluble lignin fraction was filtrated and dried to measure the weight. The overall results are summarized in Table S3.

Scanning electron microscopy (SEM). Surface and cross-section images of the mandarin peel/PVA (M/P) films were attained by a scanning electron microscope (Quattro ESEM, Thermo Scientific, United States; SU5000, Hitachi, Japan). For cross-sectional images, samples were cryo-fractured in liquid nitrogen and mounted in a cross-section sample holder. All samples were coated with platinum prior to analysis, and electron beam voltage of 10 kV was applied.

Atomic force microscopy (AFM). Surface roughness of M/P films and PVA film was examined via AFM (Park NX10, Park systems, Republic of Korea) in non-contact mode using a PPP-NCHR tip (Nanosensors, Switzerland). The arithmetic mean roughness (R_a) was calculated as the average value obtained from three distinct sampling points on each sample.

Fourier-transform infrared (FT-IR) spectroscopy. FT-IR spectrometer (Nicolet iS50, Thermo Fisher Scientific, United States) was utilized to identify the functional groups in mandarin peel powder, PVA, and M/P films (size of 1×1 cm^2). The equipment was operated in attenuated total reflectance (ATR) mode within wavenumber from 400 to 4000 cm^{-1}.

Nuclear magnetic resonance (NMR). For further compositional analysis, liquid-state ^{13}C NMR was performed using an Avance Neo 600 MHz NMR spectrometer (Bruker, United States). Mandarin peel powder, Na_2CO_3-1:1, and Na_2CO_3-1:1-W samples were chopped and immersed in DMSO-d_6 (~5 w/v%) for several days under continuous shaking. The liquid phase was then collected by centrifugation and analyzed. The obtained spectra were normalized to the DMSO solvent peak and further processed through phase correction, baseline correction, and denoising using Mnova 15.1 software (Mestrelab Research, Spain).

While PVA, pectin, and lignin are soluble in DMSO, cellulose remains largely insoluble,[3] limiting its analysis via liquid-state NMR. Additionally, solid state NMR was not feasible due to the difficulty in pulverizing the film samples. Therefore, the compositional analyses were comprehensively interpreted by integrating results from both FT-IR and NMR.

UV-Vis spectroscopy. The optical properties of M/P films were analyzed by UV-Vis/NIR spectrophotometer (Lambda 1050, Perkin Elmer, United States). M/P films (*ca.* 2.5×2.5 cm^2, 0.13–0.20 mm thick) were secured in a sample holder and analyzed in total reflectance mode over a wavelength range of 200–850 nm. The visible light transmittance was evaluated by the transmittance value at wavelength of 550 nm. UV-A and UV-B blocking percentages were obtained from the following equations (Eqn. S1 and S2).[4]

$$\text{UV - A blocking} = 100 - \frac{\int_{320}^{400} T(\lambda)d\lambda}{\int_{320}^{400} d\lambda} \quad \text{(Eqn. S1)}$$

$$\text{UV - B blocking} = 100 - \frac{\int_{280}^{320} T(\lambda)d\lambda}{\int_{280}^{320} d\lambda} \quad \text{(Eqn. S2)}$$

Tensile test. Films were cut into rectangular specimens (*ca.* 1.5×5.0 cm^2) and analyzed via a universal testing machine (Instron 5848, Instron, United Kingdom) in accordance with the ASTM 882 standard, with modifications in specimen length. This minor modification is due to practical constraints associated with the micro tensile tester and the solvent casting preparation method. The tensile test was conducted at 23 ± 1 °C temperature and 45 ± 2% relative humidity, applying a 500 N load cell and a crosshead speed of 50 mm/min. The reported values are the average calculated from at least 3 measurements.

Thermogravimetric analysis (TGA). Thermal degradation behavior of PVA, Na_2CO_3-1:1, and Na_2CO_3-1:1-W films were analyzed by a thermogravimetric analyzer (TG209 F1 Libra, Netzsch, Germany; TGA2, Mettler Toledo, Switzerland). Extrapolated onset temperatures are determined by ISO 11358-1 standard.[5]

Antioxidant ability. The antioxidant properties of the M/P films were analyzed using 2,2-diphenyl-1-picrylhydrazyl (DPPH) antioxidant assay kit (BO-DPH-200, Oxitec, United States), following the protocol provided by the manufacturer. Firstly, the M/P films (Na_2CO_3-1:1, Na_2CO_3-1:1-W), PVA film, and mandarin peel powder was immersed in 50 vol% ethanol and incubated at

37 °C for two hours. Subsequently, a 20 µL of aliquot was reacted with DPPH solution for varying durations. The radical scavenging ability at different time points was determined by measuring the absorbance at 517 nm, further calculated by Eqn. S3:

$$Radical\ scavenging\ ability\ (\%) = \frac{A_{CS} - A_S}{A_{CS}} \times 100 \qquad \text{(Eqn. S3)}$$

where $A_{cs} = A_{b1} - A_{b2}$ and $A_s = A_{sample} - A_{b2}$. The blank 1 (b1) sample contained assay buffer, ethanol, and DPPH solution, while the blank 2 (b2) sample contained only assay buffer and ethanol.

Oxygen and water vapor barrier properties. Oxygen permeability of the samples was analyzed in duplicate (except for the Na_2CO_3-1:1-W result, obtained from single measurement) via OX-TRAN Model 2/21 (MOCON, United States). Films were cut into 3×3cm^2 specimens and tested in 23 °C and 0% relative humidity per ASTM D3985 standard. Oxygen permeability (OP) of the samples were determined by the following equation:

$$OP\ (cm^3\ mm\ m^{-2}\ day^{-1}\ atm^{-1}) = \frac{OTR}{\Delta P} \times d \qquad \text{(Eqn. S4)}$$

where OTR is the oxygen transmission rate in cm^3 m^{-2} day^{-1}, ΔP is the oxygen pressure gradient across the film (*i.e.*, 1 atm), and d is the thickness of the sample (mm).

Water vapor barrier properties of the samples were analyzed in triplicate by a desiccator method illustrated in ASTM E96/E96M-24a standard with some modifications.[6] About 8 g of anhydrous $CaCl_2$ beads were placed in a 20 mL vial, and each film was sealed over the vial top using an open mouth cap (r = 15 mm). The samples then were stored in a climate chamber at 23 °C and 85% relative humidity to simulate humid conditions. After the system reaches constant

weight change rate (*i.e.*, steady state), the rate obtained from the interpolation curve was used for the calculation of water vapor permeability (WVP) by the following equation:

$$WVP\ (g\ \mu m\ m^{-2}\ day^{-1}\ Pa^{-1}) = \frac{\Delta m}{\Delta t \times A \times \Delta P} \times d \qquad \text{(Eqn. S5)}$$

where Δm is the mass change of the system (g), Δt is the time interval (day), A is the surface area of the sample (m^2), ΔP is the water vapor pressure difference across the film (Pa), and d is the thickness of the sample (μm).

Contact angle measurement. A contact angle analyzer (Phoenix 300, Surface Electro Optics, Republic of Korea) was utilized for measuring water contact angle of films in triplicate.

Water solubility test. The solubility of M/P and PVA films in 60 °C water was assessed through the following steps. First, the films were dried at 60 °C for 24 hours to remove residual moisture, and then immersed in 200 mL of 60 °C water for 24 hours. Subsequently, the retrieved films were dried again at 60 °C for another 24 hours, and the mass change was recorded. The water solubility was calculated as the ratio of reduced mass to the initial mass of the pristine sample.

Statistics. Experimental data are reported as the mean ± standard deviation from triplicate measurements, unless stated otherwise, and are generally represented by three significant figures. Results in bar graphs are provided with error bars indicating mean ± standard deviation. One-way ANOVA and Tukey's test were employed to determine significant difference between the samples using the Origin 2019 software.

Supplementary tables

Table S1. Elemental analysis for biodegradation test samples

Content (%)	Cellulose*	Na_2CO_3-1:1-W	LDPE*
Carbon	42.0 ± 0.4	50.1 ± 0.5	84.8 ± 0.35
Hydrogen	6.34 ± 0.07	8.82 ± 0.05	n.d.
Nitrogen	0	0.255 ± 0.009	n.d.
Sulfur	0	0	n.d.
Oxygen	n.d.	38.8 ± 0.0	n.d.

*Determined in the previous study;[7] n.d., not determined.

Table S2. Characteristic FT-IR peak assignments[8,9]

Wavenumber (cm^{-1})	Assignment
3300–3200	O–H stretching
2970–2900	C–H stretching
1740–1700	C=O stretching
~1600	C=C stretching (aromatic), COO^- stretching, H–O–H deformation
1600–1400	C=C stretching (aromatic), COO^- stretching
~1050	C–O–C stretching

Table S3. Compositional analysis of pectin, cellulose, and lignin in mandarin peel waste

Component	Content (%)
Pectin	13.5 ± 0.1*
Cellulose	7.1**
Lignin	8.69 ± 0.0*

* Result from duplicate experiment; **Result from single experiment.

Table S4. Summary of the mechanical and optical properties of the prepared M/P films

Sample code	Tensile properties		Optical properties		
	Tensile strength (MPa)	Elongation at break (%)	UV-A blocking (%)	UV-B blocking (%)	Transmittance at 550 nm (%)
Na_2CO_3-1:1	4.07 ± 0.50	98.2 ± 4.2	100	100	18.5
Na_2CO_3-1:2	8.61 ± 0.54	207 ± 58	N/A	N/A	N/A
Na_2CO_3-1:4	7.73 ± 0.27	309 ± 37	N/A	N/A	N/A
Delig-1:1	5.53 ± 0.63	192 ± 22	100	100	35.2
Water-1:1	5.36 ± 0.31	84.6 ± 9.1	100	100	34.6
Na_2CO_3-1:1-U	10.7 ± 0.2	64.2 ± 2.0	N/A	N/A	N/A
Na_2CO_3-1:1-W	47.9 ± 9.5	8.92 ± 0.34	95.5	99.6	63.9
Na_2CO_3-1:2-W	59.7 ± 2.6	20.4 ± 4.2	99.3	99.9	53.9
Na_2CO_3-1:4-W	54.8 ± 7.0	53.8 ± 4.3	93.2	99.3	64.0
PVA	18.5 ± 2.0	315 ± 51	14.2	21.6	91.3

N/A, Not assessed.

Table S5. Comparison of the mechanical properties and optical properties with other PVA/biomass composite film examples.

Materials	Mechanical properties		Optical properties			Ref.
	Tensile strength (MPa)	Elongation at break (%)	UV-A blocking (%)	UV-B blocking (%)	Transmittance at 550 nm (%)	
Na_2CO_3-1:2-W	59.7 ± 2.6	20.4 ± 4.2	99.3	99.9	53.9	This study
Bacterial cellulose/PVA	35.05	6.44	80.9	89.6	27.6*	[10]
PVA/cellulose	50–90	30–37	-	-	90	[11]
PVA/a-CMF	37.5 ± 0.8	221.1 ± 25.6	-	-	~80	[12]
PVA/lignin-*g*-CNF	137	~40	88.0	99.9	84.4	[13]
PVA/cottonseed shell	19.55	545.5	-	-	-	[14]
PVA/Gly-CNCs/PEDOT:PSS	65.9	320	-	-	-	[15]
PVA/nanolignin	38.1 ± 3.9	229 ± 47	~95	100	~70	[16]
PVA/nanolignin	93.7 ± 4.1	197 ± 10	100	100	~7	[17]
PVA/L-CQD	35.9 ± 1.5	~12.5	100	100	39	[18]
PVA/PVP-biochar-TiO_2 NPs	32.8 ± 0.8	625.7 ± 5.9	-	-	-	[19]

-: Not reported.; * Transmittance at 600 nm.

Note: This table is provided for reference only as the sample properties and analytical procedures may vary between studies.

Abbreviations: a-CMF, aldehyde cellulose microfiber; CNF, cellulose nanofiber; Gly, glycerol; CNCs, cellulose nanocrystals; PEDOT:PSS, poly(3,4-ethylenedioxythiophene)/polystyrene sulfonate; L-CQD; lignin-derived carbon quantum dot; PVP, polyvinylidene.

Supplementary figures

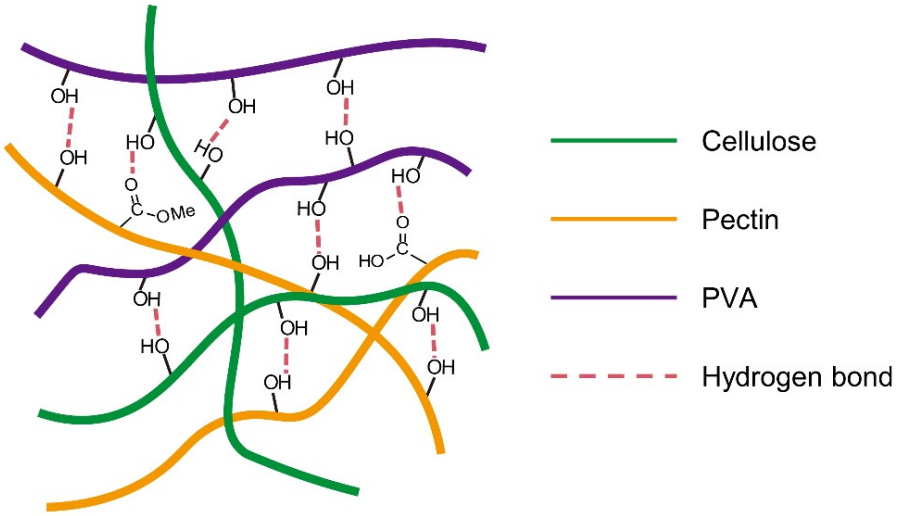

Fig. S1. Proposed structure of the mandarin peel/PVA blend films.

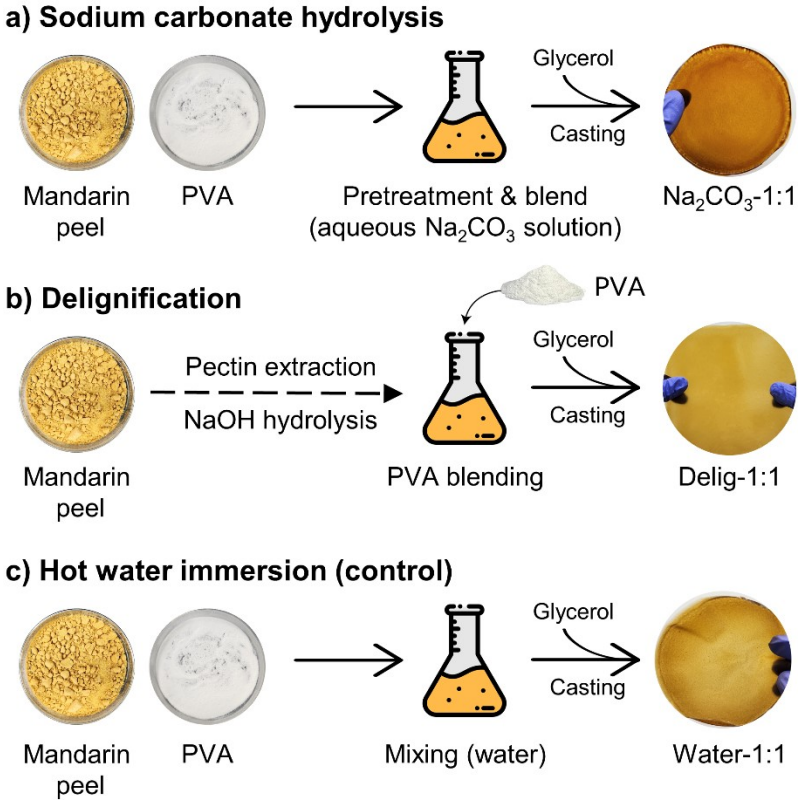

Fig. S2. Experimental scheme employing different pretreatment methods. (a) Na_2CO_3-mediated hydrolysis. (b) Delignification followed by PVA blending. (c) Hot water immersion as a control.

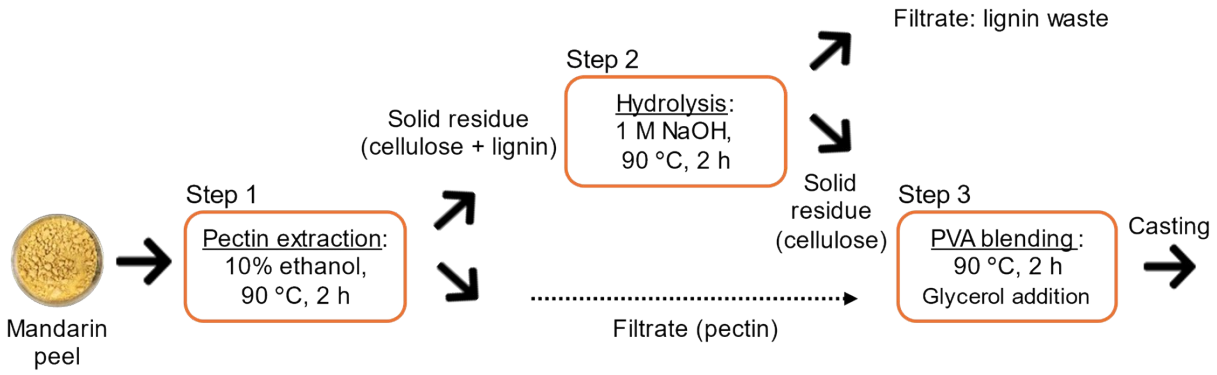

Fig. S3. Detailed procedure for Delig-1:1 sample preparation.[20]

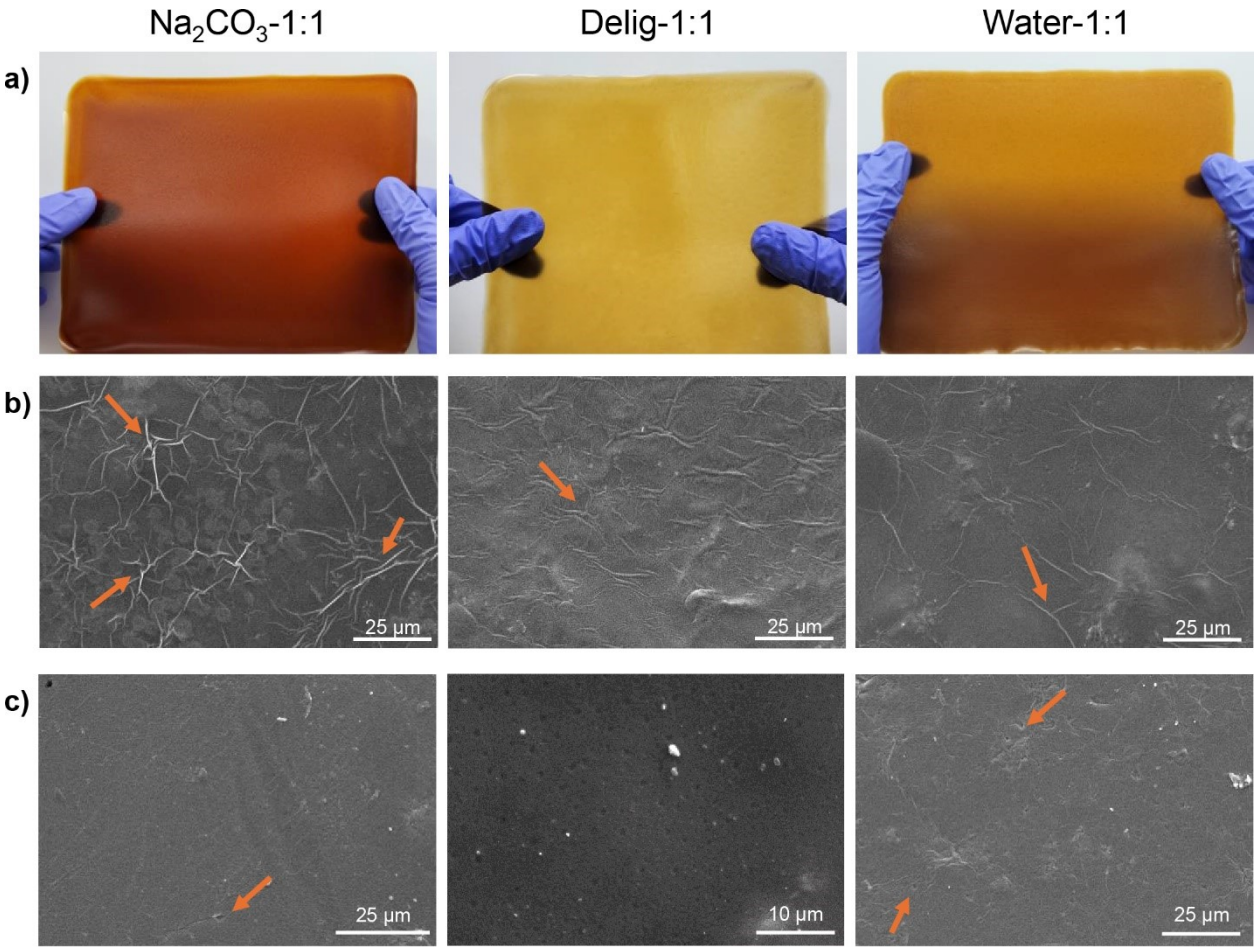

Fig. S4. Surface morphology of the blend films. (a) Digital photographs. (b) SEM images of air-contacted surface. (c) SEM images of substrate-contacted surface. Orange arrows indicate irregular surface morphology.

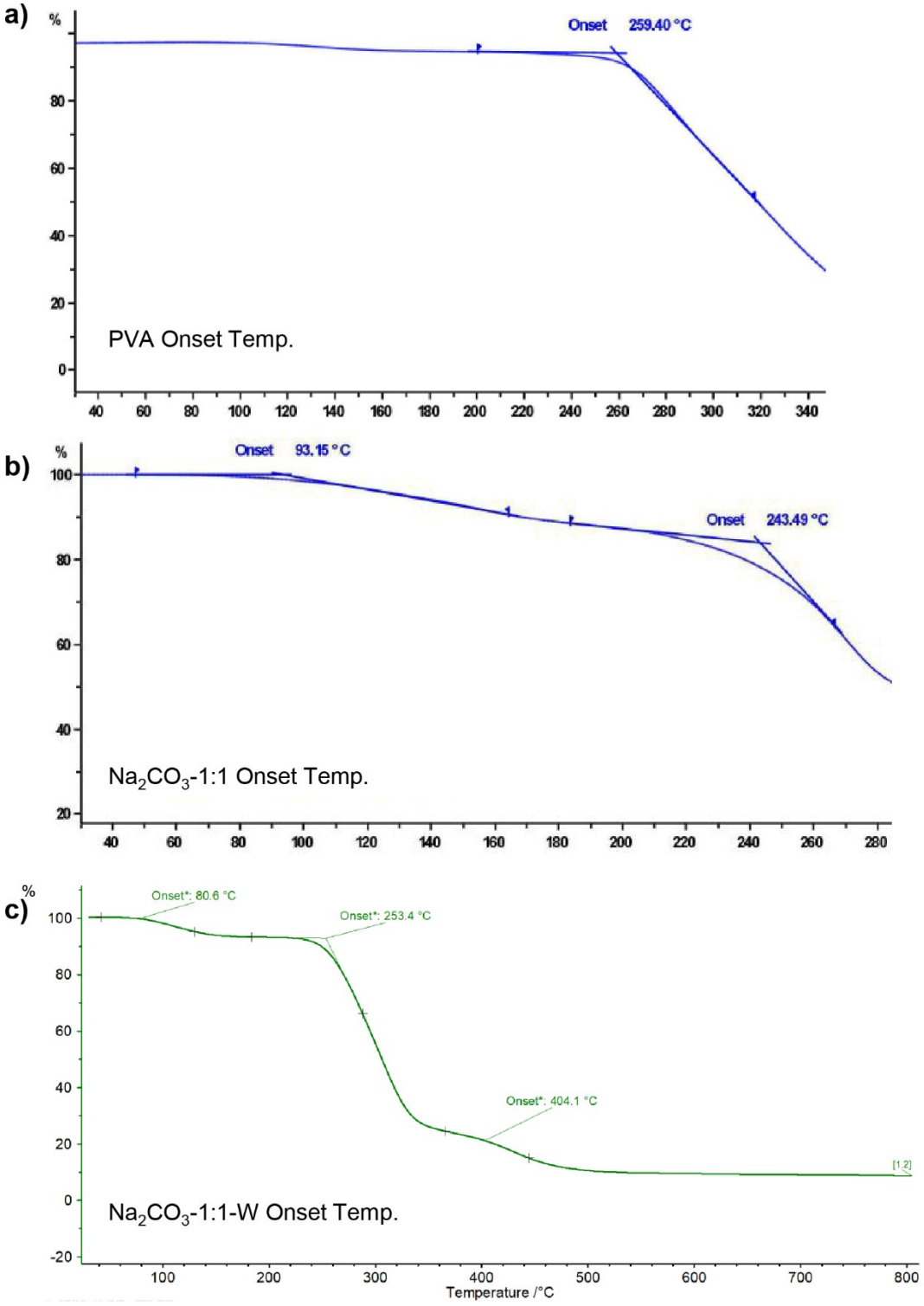

Fig. S5. Determination of onset temperatures from TGA curves. (a) PVA. (b) Na_2CO_3-1:1. (c) Na_2CO_3-1:1-W.

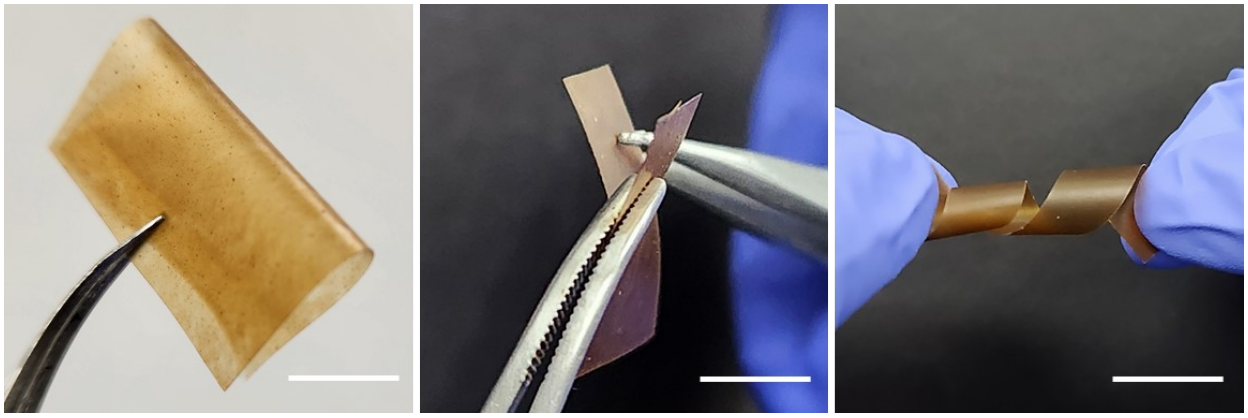

Fig. S6. Foldability and flexibility of Na_2CO_3-1:1-W film. Scale bar: 1 cm.

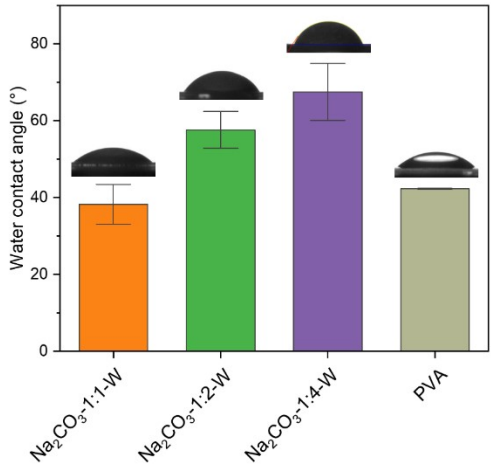

Fig. S7. Water contact angle results of M/P and PVA films.

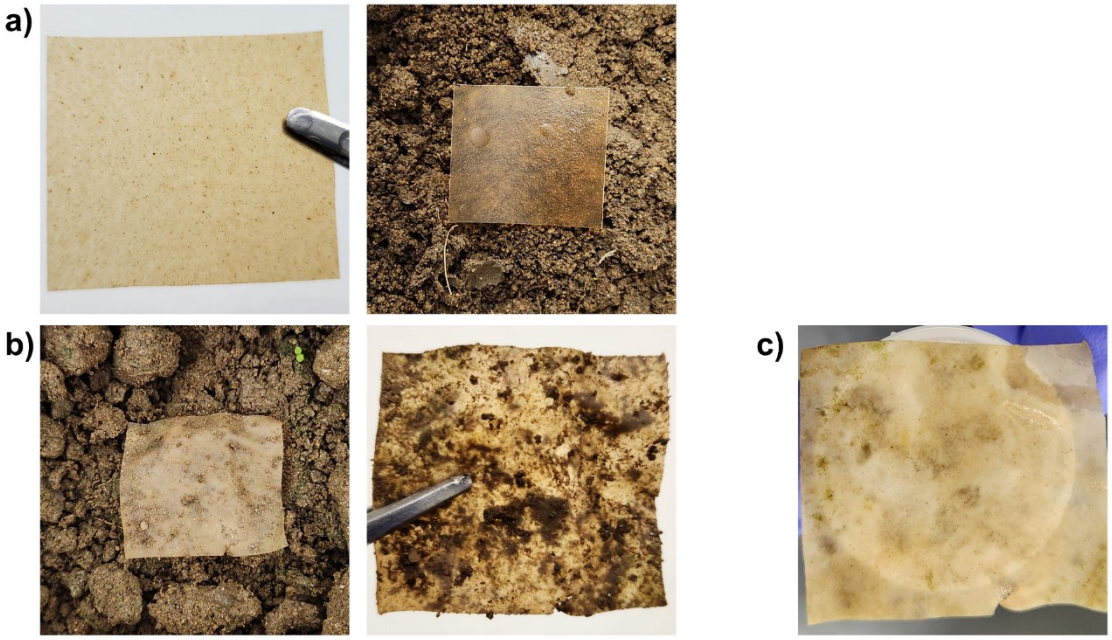

Fig. S8. Representative photos of simulated soil degradation test. (a) Initial Na2CO3-1:1-W film. (b) The film after 6 weeks of incubation. (c) The film after washing, showing microbial colonization.

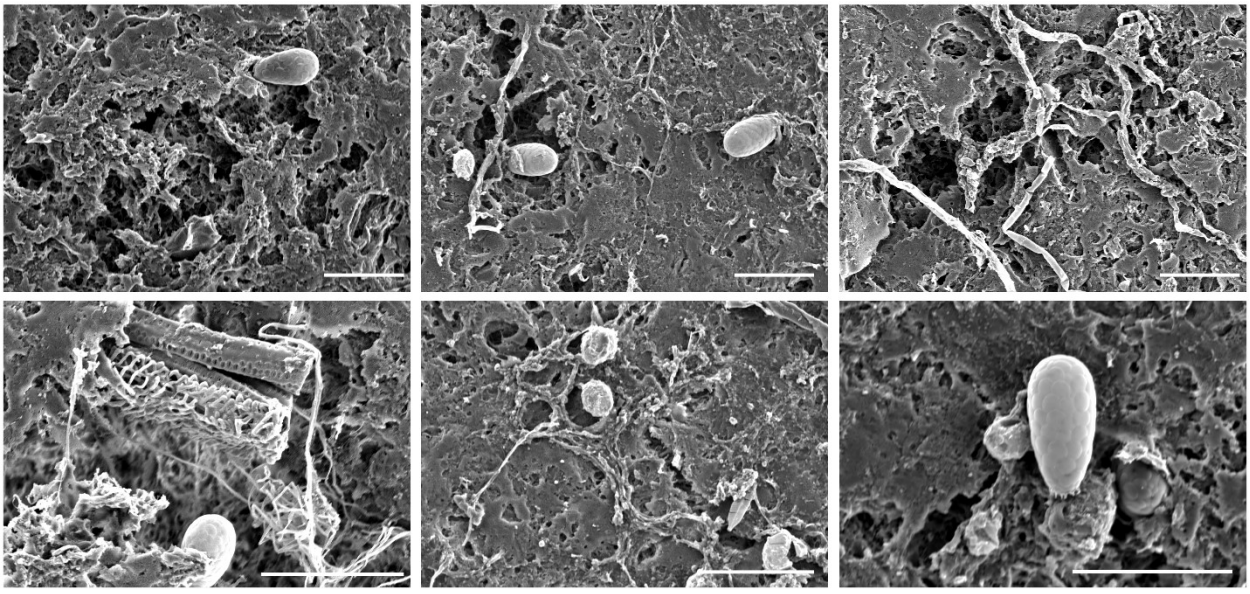

Fig. S9. Additional SEM images of Na_2CO_3-1:1-W film after 4 months of immersion in river water. Scale bar: 50 μm.

References

1. T. Wang and Y. Zhao, *Carbohydr. Polym.*, 2021, **253**, 117225. DOI: 10.1016/j.carbpol.2020.117225
2. S. Fang, X. Lyu, T. Tong, A. I. Lim, T. Li, J. Bao and Y. H. Hu, *Nat. Commun.*, 2023, **14**, 1203. DOI: 10.1038/s41467-023-36783-8
3. F. Ren, J. Wang, J. Yu, C. Zhong, F. Xie and S. Wang, *ACS Omega*, 2021, **6**, 27225-27232. DOI: 10.1021/acsomega.1c03954
4. Y. Wang, J. Su, T. Li, P. Ma, H. Bai, Y. Xie, M. Chen and W. Dong, *ACS Appl. Mater. Interfaces*, 2017, **9**, 36281-36289. DOI: 10.1021/acsami.7b08763
5. International Organization for Standardization, *ISO 11358-1:2022 - Plastics — Thermogravimetry (TG) of polymers*, Geneva, Switzerland, 2022
6. S. S. Karkhanis, N. M. Stark, R. C. Sabo and L. M. Matuana, *Composites, Part A*, 2018, **114**, 204-211. DOI: 10.1016/j.compositesa.2018.08.025
7. A. Camus, S. Choe, C. Bour-Cardinal, J. Isasmendi, Y. Cho, Y. Kim, C. V. Irimia, C. Yumusak, M. Irimia-Vladu, D. Rho, J. Myung and C. Santato, *Commun. Mater.*, 2024, **5**, 173. DOI: 10.1038/s43246-024-00592-3
8. D. Merino and A. Athanassiou, *Chem. Eng. J.*, 2023, **454**, 140171. DOI: 10.1016/j.cej.2022.140171
9. J. J. Max and C. Chapados, *J. Phys. Chem. A*, 2004, **108**, 3324-3337. DOI: DOI 10.1021/jp036401t
10. P. Cazón, G. Velazquez and M. Vázquez, *Food Hydrocolloids*, 2020, **99**, 105323. DOI: 10.1016/j.foodhyd.2019.105323
11. C. M. Zhao, X. H. Gong, X. T. Lin, C. Q. Zhang and Y. Wang, *Carbohydr. Polym.*, 2023, **321**, 121303. DOI: 10.1016/j.carbpol.2023.121303
12. Z. X. Feng, D. Xu, Z. B. Shao, P. Zhu, J. H. Qiu and L. X. Zhu, *Carbohydr. Polym.*, 2022, **296**, 119886. DOI: 10.1016/j.carbpol.2022.119886
13. M. Parit, H. S. Du, X. Y. Zhang and Z. H. Jiang, *ACS Appl. Polym. Mater.*, 2022, **4**, 3587-3597. DOI: 10.1021/acsapm.2c00157
14. G. L. Tian, L. Li, Y. J. Li and Q. Wang, *ACS Omega*, 2022, **7**, 42515-42523. DOI: 10.1021/acsomega.2c05810
15. S. C. Shi, Y. C. Hsieh and D. Rahmadiawan, *ACS Omega*, 2025, **10**, 14666-14675. DOI: 10.1021/acsomega.4c07933
16. W. J. Yang, H. Ding, G. C. Qi, C. C. Li, P. W. Xu, T. Zheng, X. M. Zhu, J. M. Kenny, D. Puglia and P. M. Ma, *Reactive & Functional Polymers*, 2021, **162**, 104873. DOI: 10.1016/j.reactfunctpolym.2021.104873
17. X. Zhang, W. F. Liu, W. Q. Liu and X. Q. Qiu, *Int. J. Biol. Macromol.*, 2020, **142**, 551-558. DOI: 10.1016/j.ijbiomac.2019.09.129

18. S. W. Park, S. H. Im, W. T. Hong, H. K. Yang and Y. K. Jung, *Int. J. Biol. Macromol.*, 2024, **268**, 131919. DOI: 10.1016/j.ijbiomac.2024.131919

19. A. Madbouly, M. Morsy and H. Moustafa, *Ceram. Int.*, 2024, **50**, 38522-38531. DOI: 10.1016/j.ceramint.2024.07.220

20. S. Zhang, Q. Fu, H. Li, P. Wu, G. I. N. Waterhouse, Y. Li and S. Ai, *Chem. Eng. J.*, 2023, **463**, 142452. DOI: 10.1016/j.cej.2023.142452